

CHAPTER-IV

SYSTEMATIC STUDY OF $B(E2; 4g \rightarrow 2g)/B(E2; 2g \rightarrow 0g)$ BRANCHING RATIO USING ASYMMETRY ROTOR MODEL AND ITS VARIATION WITH N AND Z

4.1 INTRODUCTION

The concept of collectivity in atomic nuclei is one of the most fundamental findings in history of nuclear structure physics. The macroscopic, microscopic and geometrical nuclear models have been applied to describe this collective behavior of nuclei. The geometrical models depicting the atomic nucleus as a liquid drop with a given nuclear shape and algebraic models, take into account the pairs of proton and/or neutron only. Despite the often very dissimilar theoretical approaches, most of the collective models have some common basic features, such as predictions of energies of g - band, β - band, γ - band and other higher multi-phonon bands or $B(E2)$ values and $B(E2)$ ratios for inter and intra band transitions, which have been observed in a wealth of nuclei away from closed shells.

The energy ratio $R_4 (=E_{4g}/E_{2g})$ is a key observables which can be used to assess the collectivity of nuclei and it is equal to 2.0 for an ideal spherical harmonic vibrator i.e., SU(5) limit and 3.33 in an axially symmetric deformed rotor, i.e. SU(3) limit of interacting boson model (IBM) of Iachello and Arima (1987) and Casten (1990). Bohr and Mottelson (1975) pointed out that the inter/ intra band transition rates provide another good measure of nuclear collectivity, which is less sensitive to anharmonicities than energies of various bands. The $B(E2; 4g \rightarrow 2g)/B(E2; 2g \rightarrow 0g)$ branching ratio is a particularly good example, as it is 2.0 in the spherical limit or SU(5) and 1.42 in the deformed limit or SU(3) of IBM Iachello and Arima (1987). Significant deviations from these two limiting values can be found; if one considers very small numbers of valence neutrons (N_n) and/or protons (N_p), which are used in

the IBM; also in asymmetric rotor model (ARM) of Davydov and Filippov (1958) where asymmetric parameter (γ_0) changes from 0^0 to 30^0 which corresponds to above mentioned two limits of IBM i.e. SU(3) and SU(5) respectively.

In the present chapter, we have compiled the experimental data of $B(E2;4_g \rightarrow 2_g)/B(E2;2_g \rightarrow 0_g)$ branching ratio from the website of Brookhaven National Laboratory(<http://www.nndc.bnl.gov>) for medium mass region (Nd - Hg) and listed in Table 4.1. The observed data is compared with the ARM predictions for asymmetric parameter (γ_0) equals to 0^0 to 30^0 . The SU(3) and SU(5) limits are also included to get new information about the structure. The systematic dependence of $B(E2;4_g \rightarrow 2_g)/B(E2;2_g \rightarrow 0_g)$ with N and Z are also carried out to find out a definite conclusion regarding nuclear structure.

4.2 ASYMMETRIC ROTOR MODEL

Davydov and Filippov (1958) investigated the energy levels corresponding to rotation of nucleus which does not change its internal state. They established that the violation of axial symmetry of even-even nuclei affect the rotation spectrum of axial nucleus with appearance of some new rotational states having total angular momentum of 2, 3, 4, If the deviation from axial symmetry is small, then these levels lie very high and are not excited. The energy of rotation of a non-spherical even-even nucleus is given, in the adiabatic approach, by Schrödinger eq.:

$$(H - E)\Psi = 0 \quad (4.1)$$

where E is measured in units of $\frac{\hbar^2}{4B\beta^2}$, and the operator H is given by the formula:

$$H = \frac{1}{2} \sum_{\lambda=1}^3 J_{\lambda}^2 \sin^{-2}(\gamma_0 - \frac{2\pi\lambda}{3}) \quad (4.2)$$

where J_{λ} are the projection of the total angular momentum along the axes of a coordinate system fixed in the nucleus. The wave function corresponding to the state with total moment J, can be represented as:

$$\psi_{JM} = \sum_{K \geq 0} |JK\rangle A_K \quad (4.3)$$

$$\text{where } |jk\rangle = \left[\frac{(2j+1)}{16\pi^2} (1 + \delta_{KO}) \right]^{\frac{1}{2}} \{ D_{MK}^J + (-1)^J D_{M,-K}^J \} \quad (4.4)$$

The function D_{MK}^J in eq. (4.4) is the function of the Euler angles that determine the orientation of the principal axis of the nucleus with respect to the laboratory space. It can be shown that the wave functions (4.3) from the basis of totally symmetric representation of the group D_2 , the elements of which are the rotation through 180° around each of three principal axes of the nucleus Davydov and Filippov(1958) and Davydov and Rostovsky (1959).

The values of first excited state E_{21} and second $2+$ state i.e. E_{22} can be written as (in unit of $\hbar^2/4B\beta^2$):

$$E_{21} = \frac{9 \left[1 - \sqrt{\left\{ 1 - \frac{8\sin^2(3\gamma_0)}{9} \right\}} \right]}{\sin^2(3\gamma_0)} \quad (4.5)$$

$$E_{22} = \frac{9 \left[1 + \sqrt{\left\{ 1 - \frac{8\sin^2(3\gamma_0)}{9} \right\}} \right]}{\sin^2(3\gamma_0)} \quad (4.6)$$

The value of asymmetry parameter can be obtained using the Eqs. (4.5) and (4.6) and the asymmetric parameter (γ_0) become:

$$\gamma_0 = \frac{1}{3} \sin^{-1} \left\{ \frac{9}{8} \left[1 - \left(\frac{R_\gamma - 1}{R_\gamma + 1} \right)^2 \right]^{1/2} \right\}, \text{ where } R_\gamma = \frac{E_{22}}{E_{21}} \quad (4.7)$$

4.2.1 Reduced Transition Probabilities

The reduced transition probability $B(E2; I_i \rightarrow I_f')$ between two numbers of the same rotational band with quantum number K is expressed as:

$$B(E2; I_K \rightarrow I_K') = \frac{5}{16\pi} e^2 Q_0^2 |\langle I_2 K_0 | I' K \rangle|^2 \quad (4.8)$$

where we have used

$$\sum_{m_1 m_2 m_3} |\langle I_1 I_2 M_1 M_2 | I M \rangle|^2 = (2I + 1) \quad (4.9)$$

For Coulomb excitation, the $B(E2)$, reduced transition probability in the case of symmetric rotor (even-even nuclei) is expressed;

$$B(E2; I_K \rightarrow I_K') = \frac{5}{16\pi} e^2 Q_0^2 |\langle I_{200} | I' + 2, 0 \rangle|^2$$

$$B(E2; I_K \rightarrow I_K') = \frac{5}{16\pi} e^2 Q_0^2 \frac{(I+1)(I+2)}{(2I+1)(2I+3)} \quad (4.10)$$

The non-spherical nuclei have rotational levels which are due to very fast electric quadrupole transition probability $B(E2; I \rightarrow I')$. According to equation (4.10), $B(E2;$

$I_i \rightarrow I_f$) increases as the value of intrinsic quadrupole moment Q_0 increases. If the transition takes place between the ground state ($I=0$) and the first excited state ($I=2$) of nuclei, then

$$B(E2) = \frac{5}{16\pi} e^2 Q_0^2 \quad (4.11)$$

For transition between rotational level of spin $I=2$ and $I=0$, the $B(E2)$ value can be expressed (in unit of $e^2 Q_0^2 / 16\pi$):

$$B(E2; 2_1 \rightarrow 0_1) = B(E2; 2_1 \rightarrow 0_1) / e^2 Q_0^2 / 16\pi = (1/2) \{1 + [(3 - 2\sin^2(3\gamma_0) / (9 - 8\sin^2(3\gamma_0))^{1/2})]\} \quad (4.12)$$

Where the intrinsic quadrupole moment of an axial nucleus with nuclear core deformation β is:

$$Q_0 = 3ZR^2\beta / (5\pi)^{1/2}. \quad (4.13)$$

Also the $B(E2)$ value for other transitions can be written as:

$$B(E2; 4_i \rightarrow 2_f) = 5/126 [\cos\gamma_0 (6A_{0i} A_f + \sqrt{35}A_{2i} B_f) + \sin(\sqrt{15}A_{2i}A_f + A_{0i}B_f + \sqrt{35}A_{4i}B_f)]^2$$

where, A_f and B_f are the coefficients that determine the wave functions of spin 2_1^+ and A_λ coefficients determine the wavefunction of spin 4_{1+} . Using the values of coefficients determined the wavefunctions, one can calculate the probabilities of electric quadrupole transitions between various rotational states of the nucleus. The ARM $B(E2; 4_g \rightarrow 2_g) / B(E2; 2_g \rightarrow 0_g)$ branching ratio is deduced from eqs. (4.12, 4.14) using asymmetric parameter (γ_0) from equation (4.7).

4.2.2. Calculation of Asymmetric Parameter (γ_0)

The values of asymmetry parameter (γ_0) are evaluated using eq. (4.7) by putting the the experimental energies of $E_{2_2^+}$ ($=E_{22}$) and $E_{2_1^+}$ ($=E_{21}$) states which are taken from the website <http://www.nndc.bnl.gov>. It can also be evaluated using:

(a) The energy ratio $R_4 = (E_{4g} / E_{2g})$ but only the nuclei with $2.8 \leq R_4 \leq 3.33$ will be allowed Sharma (1989) and Gupta and Sharma (1989).

(b) The $B(E2)$ values which are very small and available with uncertainties.

Therefore the values from energy ratio R_γ are more reliable. The calculated values of asymmetry parameter (γ_0) for all nuclei of medium mass region are used to calculate the $B(E2; 4_g \rightarrow 2_g) / B(E2; 2_g \rightarrow 0_g)$ branching ratio.

4.3 RESULT AND DISCUSSIONS

4.3.1 Variation of ARM $B(E2;4_g \rightarrow 2_g)/B(E2;2_g \rightarrow 0_g)$ ratio versus asymmetry parameter (γ_0)

The variation of $B(E2;4_g \rightarrow 2_g)/B(E2;2_g \rightarrow 0_g)$ ratio from ARM vs. γ_0 is shown in Fig. 4.1. The ARM data points are shown by hollow circles and the vibrational or SU(5) limit at 2.0 and rotational or SU(3) limit at 1.4 are shown by dotted lines for useful comparison. It is clear from the figure that the ARM predictions are very close to the SU(3) limiting value and also it increases very slowly on increasing γ_0 from 0° to 20° forming a peak at 20° and decreases slowly beyond 20° approaches 1.4 which is SU(3) limiting value at $\gamma_0 \approx 27^\circ$. The ARM ratio is away from vibration model limit of 2.0 this shows that it cannot explain the vibrational nature of the nuclei.

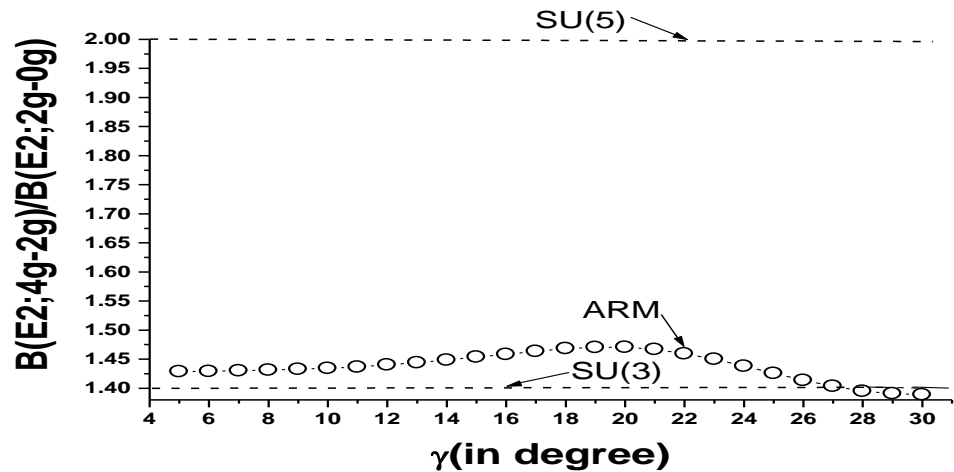


Fig.4.1 The Variation of $B(E2;4_g \rightarrow 2_g)/B(E2;2_g \rightarrow 0_g)$ ratio from ARM (shown by hollow circles) vs. asymmetry parameter (γ_0) in degree. The vibrational limit SU(5) at 2.0 and rotational limit SU(3) at 1.4 are shown by dotted lines for comparison.

4.3.1.1 Variation of Experimental and ARM $B(E2;4_g \rightarrow 2_g)/B(E2;2_g \rightarrow 0_g)$ ratio versus Asymmetry Parameter (γ_0)

The variation of $B(E2)$ ratio from experiment and ARM with γ_0 is shown in Fig.4.2. The ARM data points are shown by solid triangles and SU(5) limit at 2.0 and SU(3) limit at 1.4 are shown by dotted lines. Two nuclei are having $B(E2)$ ratio anomalously more than 2.0 and not shown in the Fig.4.2, e.g. ^{182}Hg and ^{184}Hg for them the $B(E2;4_g \rightarrow 2_g)/B(E2;2_g \rightarrow 0_g)$ ratios are 4.6(3) and 2.8(8) respectively. There are some other nuclei in medium mass region those are having this ratio anomalously lesser than 1.4 i.e. SU(3) limiting value e.g., ^{150}Nd , ^{164}Dy , ^{164}Er , ^{168}W , ^{182}W , ^{184}W , ^{192}Os , ^{180}Pt and ^{198}Hg having values 1.31(10), 1.30(7), 1.18(13), 1.1(3), 1.386(20), 1.30(9), 1.22(4), 0.92(22) and 0.375(18) respectively. It is noted that in medium mass region (Nd-Hg), this $B(E2)$ ratio is smallest in case of ^{198}Hg [=0.375(18)] which is non magic nucleus with only two vacancy of protons for $Z=82$. This ratio is also very small in case of $^{144}\text{Nd}_{84}$ [=0.73(9)]; which is also a non- magic nucleus; which has only two valence neutrons outside $N=82$. It supports the findings of Cakirli et al (2004) that the value of this $B(E2)$ ratio is anomalously small in non magic nuclei, as it cannot be explained with collective approaches. The values of $B(E2;4_g \rightarrow 2_g)/B(E2;2_g \rightarrow 0_g)$ ratios for $N=88$ isotones (Nd, Sm, Gd, Er) are lying between SU(3) and SU(5) limits indicating the shape phase transition for these nuclei. However the nature of the Dy_{88} is different and its value is close to SU(3) limit. Other data points are lying between SU(5) and SU(3) limits. While the ARM predictions are very close to the SU(3) limit.

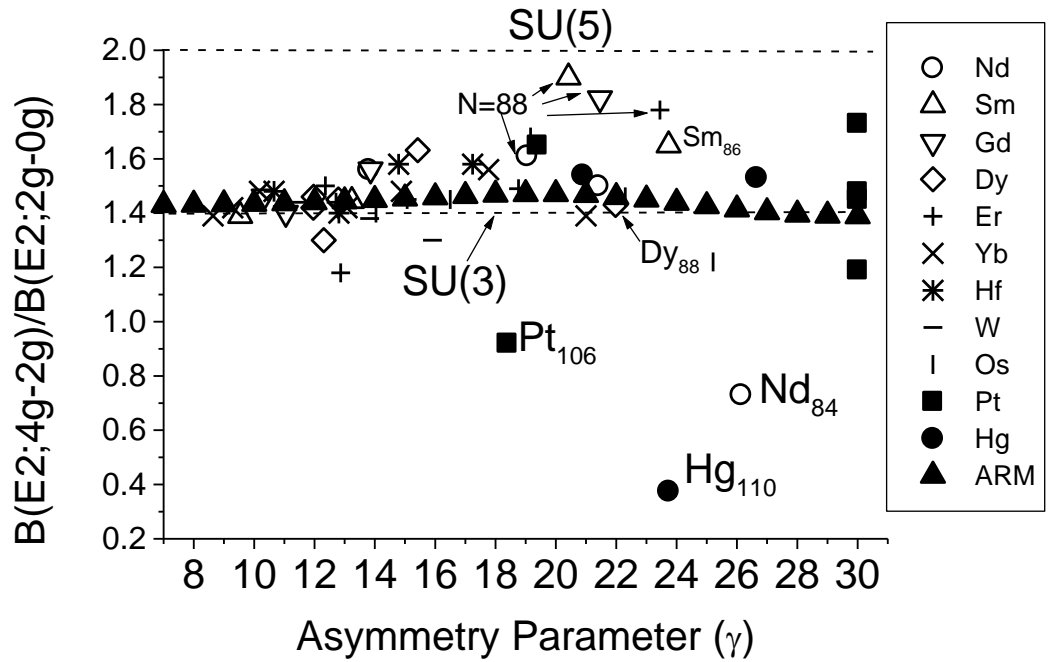


Fig.4.2 The Variation of experimental $B(E2;4g \rightarrow 2g)/ B(E2; 2g \rightarrow 0g)$ ratio vs. asymmetry parameter (γ_0) in degree. The vibrational limit SU(5) at 2.0 and rotational limit SU(3) at 1.4 are shown by dotted lines for comparison. The ratio from ARM is shown by solid triangles.

4.3.1.2 Conclusions

The predictions of asymmetric rotor model (ARM) of Davydov and Filippov(1958) for $B(E2;4g \rightarrow 2g)/B(E2;2g \rightarrow 0g)$ branching ratio are compared with the experimental data in medium mass region. It is found that the observed data point of this ratio for N=88 isotones (Nd, Sm, Gd, Er) are indicating the shape phase transition from an ideal spherical harmonic vibrator or SU(5) to an axially symmetric deformed rotor or SU(3). It is also noted that this B(E2) ratio is anomalously small in case of two non- magic nuclei i.e., $^{198}_{80}\text{Hg}_{118}$ [=0.375(18)] and $^{144}_{60}\text{Nd}_{84}$ [=0.73(9)] with only two vacancy of protons for Z =82 and two valence neutrons outside N=82, respectively; which supports the findings of Cakirli et al (2004). The data points for other nuclei are lying between SU(5) and SU(3) limits. The calculated B(E2) ratios of ARM are very close to the SU(3) limit of IBM indicating that it can

explain the structure of only well deformed nuclei. Therefore the ARM is partially successful in explaining this branching ratio.

4.3.2 SYSTEMATIC DEPENDENCE OF $B(E2; 4g \rightarrow 2g)/B(E2; 2g \rightarrow 0g)$ BRANCHING RATIO ON N AND Z

4.3.2.1 Result And Discussions

4.3.2.1.1 The variation of experimental $B(E2; 4g \rightarrow 2g)/B(E2; 2g \rightarrow 0g)$ ratio verses neutron number (N)

To avoid the overlapping of experimental data of the nuclei and to have a clear picture for a definite conclusion about the dependence of $B(E2; 4g \rightarrow 2g)/B(E2; 2g \rightarrow 0g)$ ratio on N, the whole data is divided into two parts and shown in two figures i.e. Fig. 4.3 for Nd- Er nuclei and in Fig. 4.4 for Yb- Hg nuclei. The vibrational model or SU(5) limit at 2 and rotational model or SU(3) limit at 1.4 are shown in the Fig 4.3 and Fig. 4.4. The data points are joined for same value of Z, so that the effect of N will be visible.

For Nd, this ratio increases sharply from 0.73 to 1.61(maximum value at N=88) as N increases from 84 to 88 and if N is further increased from 88 to 92 it decreases slowly from 1.61 to 1.31(see Fig. 4.3). The same feature is observed for Sm, where this ratio increases from 1.65 to 1.9 on increasing N from 86 to 88 and beyond N=88 it drops sharply and approaches to Alaga value of 1.4 for N=92. In case of Gd, the BE(2) ratio decreases from 1.82 to 1.46 as N increases from 88 to 94. Also in Er, this ratio decreases from 1.78 to 1.5 as N increases from 88 to 100 and minimum value of 1.18 at N=96. Therefore, for N=88 (Sm, Gd and Er) isotones, this ratio ≈ 1.8 is very close to the VM limit of 2.0 indication vibrational nature. However for Dy (N=88, 92, 94, 96) this ratio is close to Alaga value indication deformed rotor nature and for N=90; Dy indicating transitional nature because this ratio (=1.63) is lying in between SU(5) and SU(3) limiting value (see Fig. 4.3).

For Yb and Hf nuclei, BE(2) ratio is ranging between 1.4 to 1.6 for different values of N and close to SU(3) limit (see Fig. 4.4). In case of W, the ratio increases sharply from 1.1(3) to 1.74(15) on increasing N from 94 to 100 and decreases very slowly on increasing N from 108 to 112 (almost remains around Alaga value).

For N=96 the data point of Os is close to the other N=96 isotones (Yb, Hf, W) data points. When N increases from 108 to 112, the ratio for Os increases from 1.4(4) to 1.68(11) and when N is increased from 112 to 116 the B(E2) ratio decreases from 1.68(11) to 1.22(4) indicating prolate to oblate shape-phase-transition as observed by Kumar and Baranger (1968).

For N=98, the B(E2) [=1.87(24)] for Pt is close to VM value and for N=102 the ratios is minimum [=0.92(22)]. The B(E2) ratio for Pt decreases from 1.65 to 1.56 when N increases 106 from 114 and again increases from 1.56 to 1.73 as N increases from 114 to 116(attains maximum value =1.73(11) at 116). If N is increased from 116 to 120 this ratio drops linearly with the same slope as observed for Os (N=112 to 116). This indicates the similar nature of Pt and Os nuclei for this region.

For two nuclei; ^{182}Hg and ^{184}Hg ; the B(E2) ratio is 4.6(3) and 2.8(8) respectively; which are anomalously more than VM limiting value and not included in the Fig.2. The B(E2) ratio is smallest in case of ^{198}Hg ; which is non magic nucleus; has only two vacancy of p+ for Z =82. This ratio is also very small in case of $^{144}\text{Nd}_{84}$ [=0.73(9)] (see Fig.4.3); which is also a non- magic nucleus; which has only two valence n^0 outside N=82. It supports the findings of Cakirli et al. (2004), that the B(E2;4g \rightarrow 2g)/B(E2;2g \rightarrow 0g) ratio is anomalously small in non magic nuclei, as it cannot be explained with collective approaches.

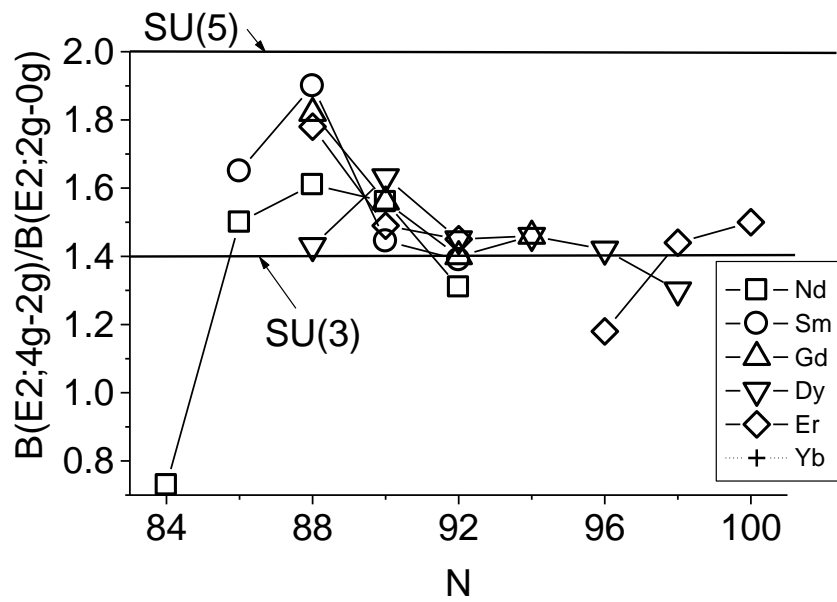


Fig.4.3: The variation of experimental $B(E2;4g \rightarrow 2g)/B(E2;2g \rightarrow 0g)$ ratio vs. neutron number (N) for Nd- Er nuclei. The vibrational limit SU(5) at 2.0 and rotational limit SU(3) at 1.4 are shown by dotted lines for comparison.

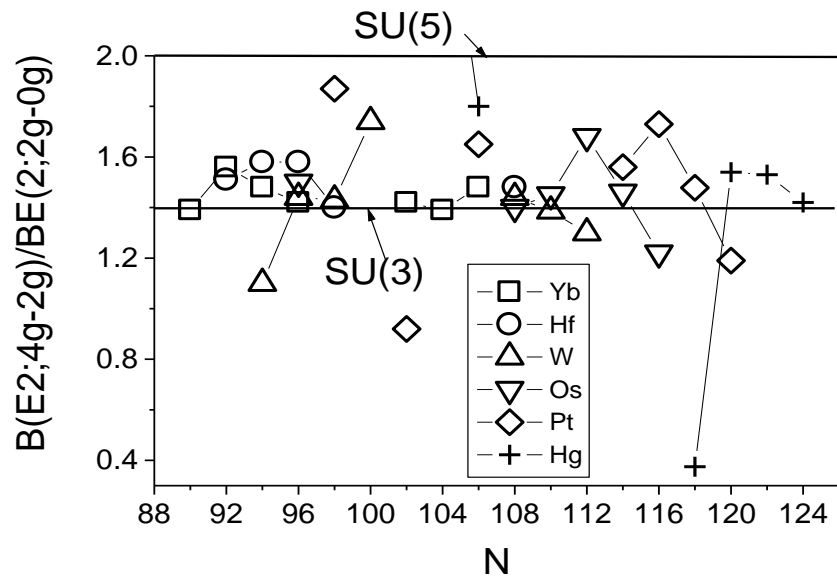


Fig.4.4: The variation of experimental $B(E2;4g \rightarrow 2g)/B(E2;2g \rightarrow 0g)$ ratio vs. neutron number (N) for Yb- Hg nuclei. The vibrational limit SU(5) at 2.0 and rotational limit SU(3) at 1.4 are shown by dotted lines for comparison.

4.3.2.1.2 The variation of experimental $B(E2;4g \rightarrow 2g)/B(E2;2g \rightarrow 0g)$ ratio versus proton number (Z).

The variation of observed $B(E2;4g \rightarrow 2g)/B(E2;2g \rightarrow 0g)$ ratio with proton number (Z) is shown in Fig. 4.5, 4.6 and 4.7 for N=84 to 92, N=94 to 102 and N=104 to 124 isotones respectively and the experimental points are joined for same value of N to observe the effect of Z. The vibrational limit (VM) or SU(5) at 2 and rotational limit or SU(3) at 1.4 are also shown by dotted lines for useful comparison in each figure.

It is evident from Fig. 4.5, that the BE(2) ratio for N=88 isotones increases on increasing Z from 60 to 62 (attains the maximum values for Sm_{88}) and decreases for Gd and Dy (attains minimum value close to SU(3) limit for Dy_{88}) and again for Er it increases. For N=88, the B(E2) ratio is close to SU(5) limiting value for Sm, Gd and Er while Dy reflects SU(3) nature and Nd in between these two limits. Also, the Sm_{88} is least deformed and Dy_{88} is most deformed. For N=86 isotones the B(E2) data is available only for two nuclei and it is increasing on increasing N from 60 to 60 as in the case of N=88.

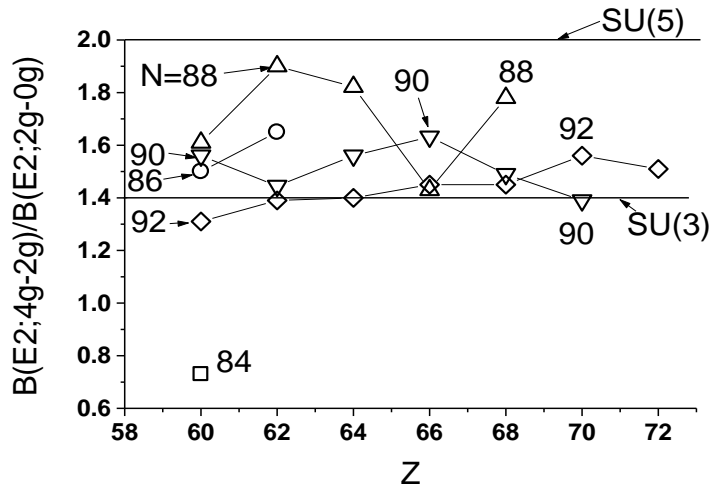


Fig.4.5: The variation of experimental $B(E2;4g \rightarrow 2g)/B(E2;2g \rightarrow 0g)$ ratio vs. proton number (Z). The vibrational limit SU(5) at 2.0 and rotational limit SU(3) at 1.4 are shown by dotted lines for comparison. The experimental points are joined for same value of N to observe the effect of Z on this B(E2) ratio for each isotones for N=84-92.

For N=90 isotones the behavior of B(E2) is just opposite to N=86 and 88; the B(E2) ratio initially decreases as N increases from 60 to 62 and increases as N increases from 62 to 66 just opposite to N=88. It is evident from the figure that the gap is maximum between the two curves for N=88 and 90 around Z= 64 indication the subshell effect at Z=64 for N<90. It is supporting the findings of Casten (1985) and Casten and Zamfir (1996).

In general, for N=90 isotones, the B(E2) ratio is somewhat independent of Z indicating constant structures because the values of this ratio are ranging between 1.45 to 1.6 and it support the findings of Gupta (2012). For N=90 isotones, this B(E2) ratio initially decreases on increasing Z from 60 to 62 (attains minimum values which is close to SU(3) limiting value for Sm₉₀ unlike Sm₈₈ for which this ratio is close to SU(5) limiting value) and increases slowly on increasing Z from 62 to 66; and attains maximum value(=1.6) for Dy₉₀; and beyond Z=66 the BE(2) decreases linearly on increasing Z from 66 to 70 (and approaches 1.4 value for Hf₉₀). It is clear from Fig. 4.5 that Sm₉₀ and Hf₉₀ are most deformed in comparison to other N=90 isotones.

For N=92 isotones, this ratio goes on increasing very slowly from 1.31 to 1.56 on increasing Z from 60 to 74 and is close to SU(3) limiting value of 1.4. However for N=94, this ratio is almost constant because its values are 1.46±0.05, 1.46±0.07, 1.48±0.07, 1.58±0.10 and 1.1±0.3 for Gd, Dy, Yb, Hf and W isotopes respectively indication Z independency. For N=94, 96 and 98 isotones (see Fig. 4.6) the ratio is close to SU(3) limiting value indicating deformed nature. For other isotones the B(E2) ratio is lying between SU(5) and SU(3) or O(6) limiting values (see Fig. 4.7) as predicted by the asymmetry rotor model Sharma and Kaushik (2015a).

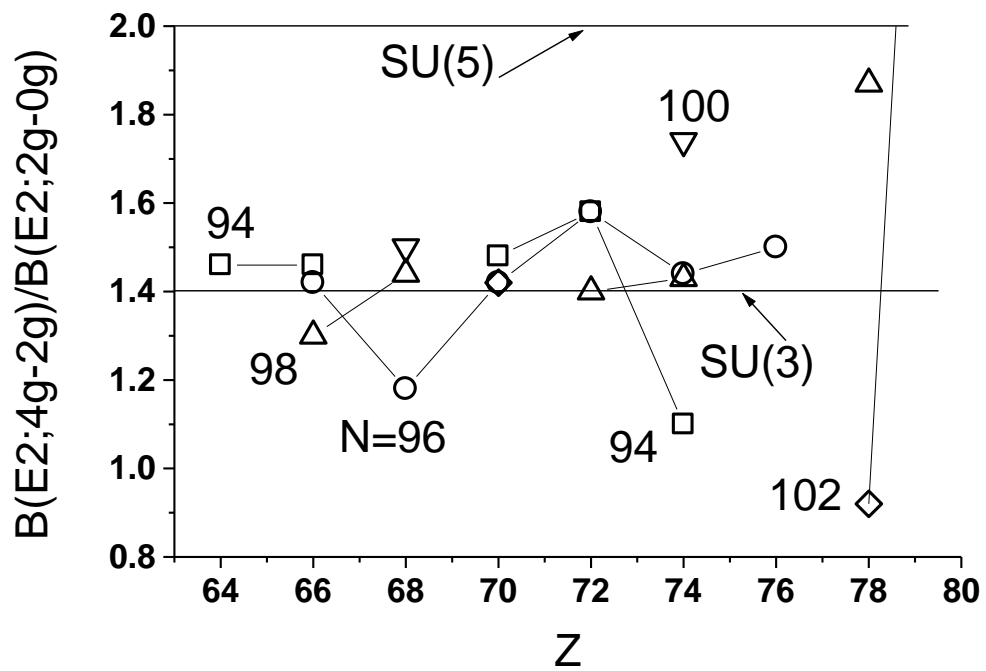


Fig.4.6: Same as Fig.3 for $N=94$ to 102 .

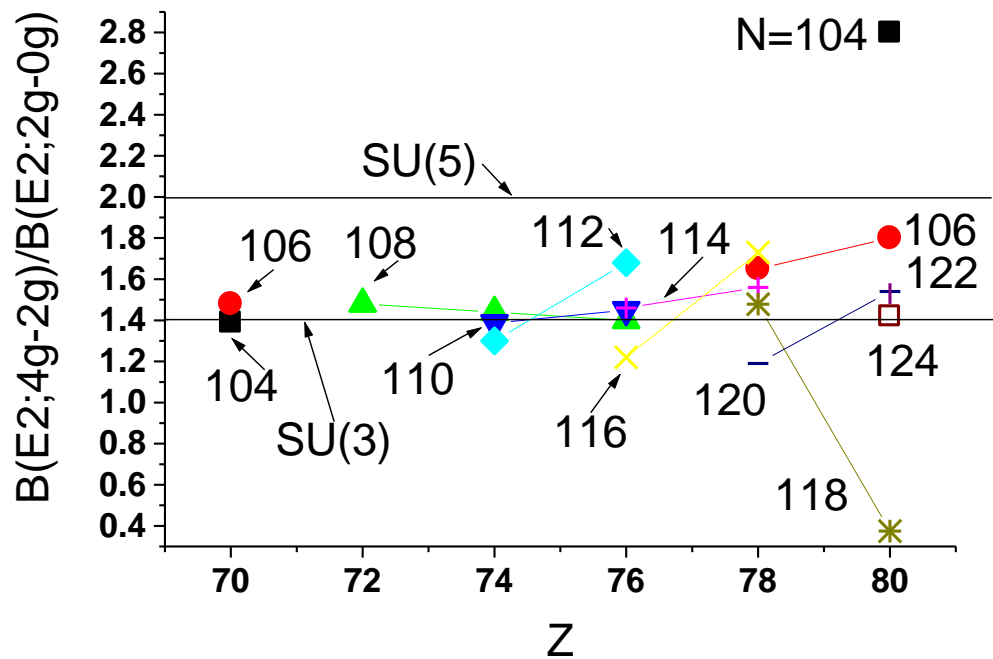


Fig.4.7: Same as Fig.3 for $N=104$ to 124 .

4.3.2.1.3 Conclusion

The variation of $B(E2; 4g \rightarrow 2g) / B(E2; 2g \rightarrow 0g)$ ratio with N and Z is shown for Nd – Hg nuclei. It is found that there is shape phase transition for N=88 and 90 isotones (Nd, Sm, Gd, Er) from an ideal spherical harmonic vibrator or SU(5) to an axially symmetric deformed rotor or SU(3). Also B(E2) ratio is anomalously small for two nuclei i.e., $^{198}_{80}\text{Hg}_{118}$ ($=0.375 \pm 0.018$) and $^{144}_{60}\text{Nd}_{84}$ ($=0.73 \pm 0.090$) with only two vacancy of p+ for Z =82 and two valence n⁰ outside N=82, respectively; which supports the findings of Cakirli et al. (2004). The present study supports the subshell effect around Z=64, for N ≤ 90 as observed by Casten (1985) and Casten and Zamfir (1996). The $B(E2; 4g \rightarrow 2g) / B(E2; 2g \rightarrow 0g)$ ratio for N=90 isotones is almost constant indicating that the nuclear structure is constant for these nuclei and it is supporting the findings of Gupta (2012). Partial results have been published recently Sharma and Kaushik (2015a, 2015b).

Table 4.1: The experimental values of $B(E2; 4g \rightarrow 2g) / B(E2; 2g \rightarrow 0g)$ branching ratio taken from <http://www.nndc.bnl.gov>. The error is also mentioned with each value after a gap shown by *italic*.

A	Nd	Sm	Gd	Dy	Er	Yb	Hf	W	Os	Pt	Hg
Z	60	62	64	66	68	70	72	74	76	78	80
144	0.73 9										
146	1.5 4										
148	1.61 9	1.65 21									
150	1.56 4	1.9 3									
152	1.31 10	1.445 22	1.82 2								
154		1.39 3	1.56 6	1.43 15							
156			1.40 3	1.632 24	1.78 12						
158			1.46 5	1.45 10	1.49 8						
160				1.46 7	1.45 8	1.39 14					
162				1.42 6		1.56 8					
164				1.30 7	1.18 13	1.48 7	1.51 22				
166					1.44 6	1.42 9	1.58 10				
168					1.50 5		1.58 11	1.1 3			
170							1.4 4	1.44 15			
172						1.42 10		1.43 16	1.50 17		
174						1.39 7		1.74 15			
176						1.48 15				1.87 24	
178											
180							1.48 20		1.6 5	0.92 22	
182								1.44 8			4.6 3
184								1.386 20	1.4 4	1.65 9	2.8 8
186								1.30 9	1.45 7		1.8 8
188									1.68 11		
190									1.46 9		
192									1.22 4	1.56 9	
194										1.73 11	
196										1.478 23	
198										1.19 13	0.375 18
200											1.54 3